*J Mater Sci* (2018) 53:8978–8988

## Composites

# High thermal conductivity of diamond/copper composites produced with Cu–ZrC double-layer coated diamond particles

Yanpeng Pan[1], Xinbo He[1,*], Shubin Ren[1], Mao Wu[1], and Xuanhui Qu[1]

[1] Institute for Advanced Materials and Technology, University of Science and Technology Beijing, 30 Xue Yuan Road, Beijing 100083, People's Republic of China


**Received:** 11 December 2017
**Accepted:** 27 February 2018
**Published online:** 9 March 2018

© Springer Science+Business Media, LLC, part of Springer Nature 2018


## ABSTRACT

A new method was proposed to fabricate diamond/Cu composites. Double-layer diamond particles were directly compressed at ultra-high pressure to prepare the preform and then sintered in a vacuum equipment for densification. The raw diamond particles were coated with zirconium carbide by magnetron sputtering for the inner layer and then deposited with copper by chemical method for the outer layer. Prepared with these particles, the composites had good interface bonding and homogeneously distributed particles in the copper matrix. The thermal conductivity of 65 vol% diamond/Cu composite was as high as 720 W $m^{-1}$ $K^{-1}$. When the diamond content increased to 70 vol%, the coefficient of thermal expansion was extremely low ($4.33 \times 10^{-6}$/K). With superb thermal–physical performance, diamond/Cu composites are potentially applicable to electronic packaging.


## Introduction

Electronic packaging material has been researched for many years, and traditional materials, such as W–Cu, $SiC_p$–Al and $SiC_p$–Cu, no longer satisfy the cooling requirements of microelectronic circuit board with high integration degree or energy-intensive laser equipment [1, 2]. As diamond has the highest thermal conductivity (1300–2300 $Wm^{-1}$ $K^{-1}$) and exceptionally low coefficient of thermal expansion, it is feasible to be composited with copper matrix for electronic packaging applications [3, 4].

Diamond/Cu composites are fabricated mainly by two methods: powder metallurgy and infiltration. As a simple and easy method, powder metallurgy usually produces composites by pressurized sintering of a mixture of copper and diamond powders with specific devices, such as spark plasma sintering [5–7], vacuum hot pressing [8–11], high-temperature high-pressure process [12] and pulse plasma sintering [13]. Composites are commonly sintered under the melting point of copper or copper alloy to prevent the matrix metal from flowing out from graphite die at a high pressure. However, the interface bonding of diamond surface with solid powders is inferior to

Address correspondence to E-mail: xb_he@163.com

Springer

https://doi.org/10.1007/s10853-018-2184-9

that with liquid metal even if diamond is coated with interface layer. Moreover, since physical properties, especially density and granularity, differ largely, it is difficult to produce diamond/Cu composites with high volume fractions owing to uneven blending of the powders. Both factors limit applications of the composites. In contrast, infiltration allows molten metal to penetrate the diamond preform to fabricate diamond/Cu composites with high volume fractions [14–20]. There are both pressure and pressureless infiltrations. Due to the capillary effect, copper alloy liquid infiltrate into the gaps between diamond particles. Meanwhile, the diamond particles disorderly stack in the infiltration preform, and some gaps (sharp angle and adhesive faces of diamond particles) are hardly saturated without pressure. Therefore, high infiltration temperatures (1250–1450 °C) were selected to reduce the viscosity of liquid metal during pressureless infiltration [14]. And copper alloy rather than pure copper was employed as the infiltration metal, which reduced the thermal conductivity of the matrix. Auxiliary pressure infiltration uses sophisticated device to apply external pressure, such as gas [15–17] and mechanic pressure [18–20], so molten metal penetrates the diamond preform, giving the best thermal properties up to now [16]. Regardless, all the infiltration methods need to prefabricate a diamond preform before permeation. When pressure is applied to assist molten metal to permeate the preform, the residual binder therein decomposes and disappears, thereby rearranging diamond particles and severely affecting the dimensional accuracy. Meanwhile, to avoid uneven rearrangement, the infiltration thickness of preform should be moderate. Therefore, a secondary process is in need. However, the composites are difficult to be machined because of the ultra-high hardness of diamond and the cost-prohibitive laser. All these factors restrict the production of diamond/Cu composites with complex shapes, so they have seldom been applied in the electronic packaging field.

Based on the methods discussed above, we proposed a new way to fabricate diamond/Cu composites with excellent thermal properties. Double-layer diamond particles, as raw material, were put into a stainless steel mould to fabricate composite preform at ultra-high pressure, and then sintered into a graphite mould with corresponding size under vacuum. Ti, Cr, Zr, Mo, W and B elements can improve the wettability between diamond and copper, among which Zr is most effective, and the corresponding composites have the highest thermal conductivity so far [16]. In this study, diamond particles were coated with zirconium carbide by magnetron sputtering to improve the wettability between the diamond surface and copper matrix. Then copper was deposited onto the zirconium carbide layer by electroless plating many times. The copper layer was thick enough and could be compressed to replace copper powders as the matrix. In this way, the powder mixing step was eliminated, and diamond particles were no longer unevenly distributed. As a result, diamond/Cu composites with high volume fraction were easily prepared. As the double-layer diamond particles can be loaded into a mould with arbitrary shapes and without segregation, they can be used to form complex parts impossible to be fabricated through infiltration.

## Experimental

MBD8-grade synthetic diamond with integral crystal structure of 100 μm was purchased from Polaris Diamond Powder Co., Ltd. The crystallized diamond particles with regular octahedral or polyhedral morphology had higher thermal conductivity, which became spherical particles when the copper layer with a specific thickness was deposited. The spherical double-layer diamond particles were densely stacked when loaded into the mould, benefiting the densification of diamond/Cu composite.

The diamond particles were coated with zirconium by magnetron sputtering. Through controlling the deposition temperature and time, zirconium with a certain thickness was deposited onto the raw diamond surface. In order to ensure the shadow surface of diamond particle was coated with zirconium, a rotary device was used for placement. In the process of magnetron sputtering, each facet of diamond particle was completely coated by zirconium through movement of the rotary device at a uniform speed. High-purity zirconium (99.9 wt%) was used as the target material for sputtering. To ensure the bonding property of coating, the diamond surface was cleaned in ethanol for 10 min with ultrasonication. Before magnetron sputtering, the chamber was pumped to low vacuum ($1 \times 10^{-3}$ Pa). Then high-purity argon (99.999%) was introduced as the working gas. During magnetron sputtering, the furnace temperature was

kept at 200 °C for 10 min. In the presence of an intense magnetic field, the zirconium atoms were sputtered onto the diamond surface by bombarding target with $Ar^{+}$. Then the diamond particles were heat-treated at 700 °C for 30 min in vacuum atmosphere to form a thin zirconium carbide layer between diamond surface and zirconium. To ensure the plating uniformity, a small amount of diamond powders (20 g) were spread evenly. An over-thick coating layer increased the interfacial thermal resistance, but an over-thin one generated deposition or coating flaws leading to direct contacting of the raw diamond with copper matrix.

Then copper was deposited onto zirconium carbide-coated diamond particles by electroless plating. The diamond surface was sensitized by $Sn^{2+}$ in a solution of 50 ml $L^{-1}$ HCl and 20 g $L^{-1}$ $SnCl_2$ and then activated by $Pd^{2+}$ in a solution of 20 ml $L^{-1}$HCl and 0.35 g $L^{-1}$$PdCl_2$. Diamond powders were agitated as a suspending liquid with a magnetic stirrer thoroughly exposed to the solution. A specific electroless copper bath was prepared: 10 ml·$L^{-1}$ 37 wt% aqueous HCHO solution, 14 g $L^{-1}$ $C_4O_6H_4KNa$, 14.5 g $L^{-1}$ EDTA and 15 g $L^{-1}$ $CuSO_4{\cdot}5H_2O$. By titrating with aqueous solution of NaOH, the pH value was kept within 12.5–13.5. The temperature was controlled between 43.5 and 45 °C during plating. To ensure that each diamond particle was plated with copper, calculated grams of diamond powders were tiled as a single layer at the bottom of the beaker in the first electroless copper deposition process. After the diamond surface was coated with a thin copper layer, the particles were transferred to copper plating bath with magnetic stirring to thicken the copper layer. After deposition many times, the diamond particles were deposited with copper of enough thickness, yielding double-layer particles with 50, 55, 60, 65 and 70 vol% diamond contents. To obtain the designed volume fractions of the diamond, precise quantitative reagents were prepared during electroless plating. A specified quality of diamond powders was coated with copper in a specified volume of copper electroless plating bath. $Cu^{2+}$ (provided by $CuSO_4$) was completely plated onto the surface of diamond particles when the plating time was long enough. After plating, the weight gain of diamond particles was calculated to verify the volume fraction of diamond, and the composite with corresponding volume fraction of diamond was obtained after compression and sintering.

Diamond/Cu preform with particular diamond volume fraction was made by compressing the double-layer diamond particles at ultra-high pressure (1.2 GPa). To prevent deformation of the diamond/Cu preform during sintering, a graphite mould with corresponding size was used to load the sample. Without pressure, the diamond/Cu composites were sintered at 1100 °C for 1 h under vacuum for densification. When the sintering temperature exceeded the melting point of copper, the liquid copper filled microscopic pores in the preform more easily. Besides, the outer zirconium layer readily spread into the liquid copper and a thin ZrC layer resided, which dramatically reduced the interfacial thermal resistance.

The fracture surfaces were observed by scanning electron microscope (SEM) with JSM-6510A scanning electron microscope, and element distribution at the interface was detected by energy-dispersive X-ray spectroscopy (EDS). The phases of coating layers were analysed by X-ray diffraction (XRD) using D5000 Siemens X-ray diffractometer. The Archimedes' law was utilized to measure the composite density. Thermal diffusivity and specific heat were measured by Netzsch LFA 427 transient Laser Flash machine and calorimetric technique, respectively. By multiplying the composite density, thermal diffusivity and specific heat, the thermal conductivity was obtained.

## Results and discussion

Figure 1a, b shows the SEM images of raw diamond particles with consistent granular size and regular contour for each one. After coating diamond with zirconium by magnetron sputtering, a very thin zirconium layer was deposited onto the diamond surface (Fig. 1c, d). Both {100} and {111} planes are smooth without raised or depressed areas, ensuring even heat transmission near the interface between diamond and copper. Figure 1e, f shows copper deposition onto the zirconium layer. By repeated electroless plating with small quantities, uniform and near-spherical double-layer particles were obtained. The surface of copper coating layer was slightly subjected to bumps and uplift, which can be ascribed to the fluctuation of $CuSO_4$ concentration in the plating bath. Nevertheless, the bumps did not

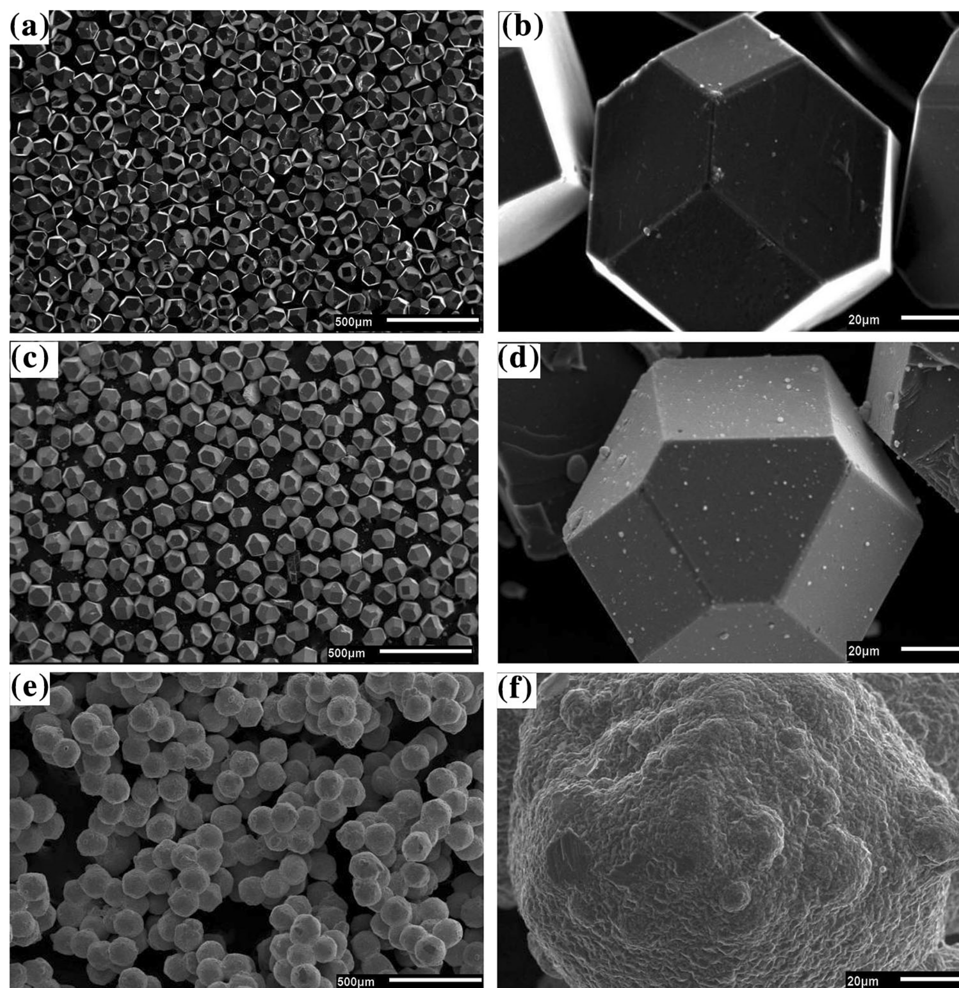


**Figure 1** Morphology of **a**, **b** raw, **c**, **d** zirconium carbide-coated and **e**, **f** copper-deposited diamond particles.

influence the properties of the composite with controllable sizes.

Figure 2 shows the XRD patterns of zirconium carbide-coated and raw diamond particles. The weak peaks of zirconium indicate low amount of coating and thin coating layer on the diamond surface. There are peaks of zirconium carbide and pure zirconium, so zirconium reacted mildly with the surface of trace graphitized diamond to form zirconium carbide during heat treatment. After forming zirconium carbide as the inner layer, copper was plated as the outer layer to form double-layer particles, with the XRD pattern shown in Fig. 3. Through electroless plating stepwise, the diamond inner layers were slowly covered with copper, and the copper peaks gradually replace those of diamond and zirconium. As shown in Fig. 3e–g, when diamond was coated with 10, 20 and 30 vol% copper, trace ZrC and Zr peaks can be identified. However, with increasing plating thickness, these peaks vanish. The peaks of diamond also

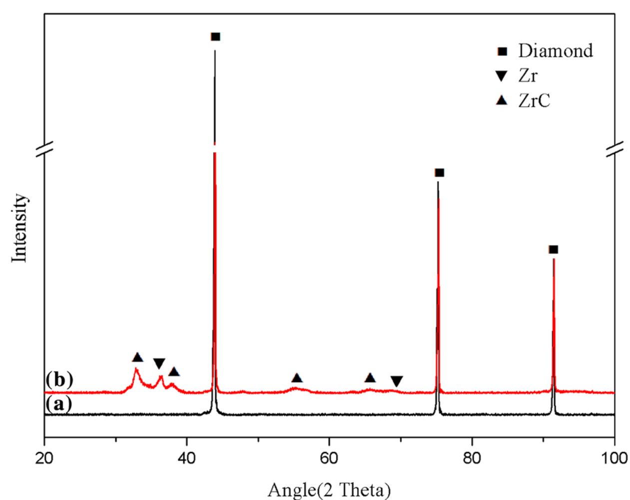


**Figure 2** XRD patterns of *a* raw and *b* zirconium carbide-coated diamond particles.

reduce significantly when the copper content exceeded 40 vol%. As to the diamond particles containing

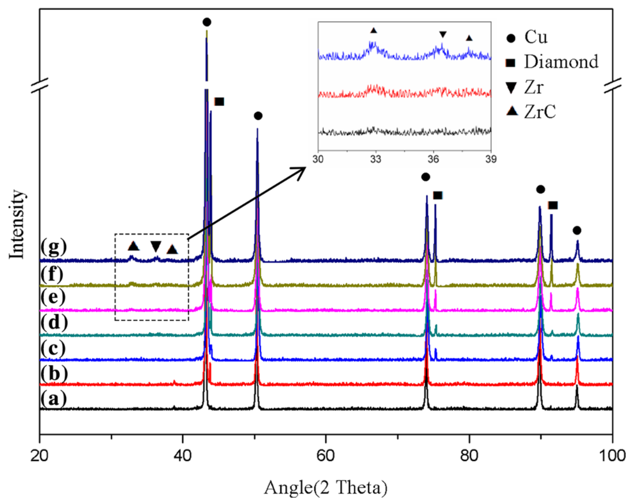


**Figure 3** XRD patterns of copper-deposited diamond particles: *a* 50 vol%, *b* 55 vol%, *c* 60 vol%, *d* 65 vol%, *e* 70 vol%, *f* 80 vol% and *g* 90 vol% diamond–copper particles.

45–50 vol% copper, the surface was covered with copper completely, so only copper peaks can be detected (Fig. 3a, b).

Figure 4a, b shows the macroscopic fracture surface of diamond/Cu composites fabricated with double-layer coated diamond particles. The diamond particles were uniformly distributed in the copper matrix, without segregation, mainly because the copper powder mixing process was replaced by copper plating. Diamond bounds copper tightly, and diamond particles were barely extracted from the copper matrix. As the coated diamond particles strongly contacted with copper, plastic fracture occurred within the copper matrix and copper adhered to diamond. The plastic fracture happened only when the interfacial bonding strength in the composites was higher than the fracture strength of copper matrix [15]. Besides, micro-cracks existed on the surface of some synthetic diamond particles and ultra-high cold pressure (1.2 GPa) aggravated the spread of the micro-cracks. With applying the shear stress along the cracks, transgranular fracture of diamond tended to occur when the bonding strength of the interface was higher than the particle fracture stress. Collectively, the diamond particles had strong interface binding and homogeneous distribution.

Figure 5a shows the EDS line-scanning analysis across the interface between diamond with transgranular fracture and the copper matrix. With increasing scan path, the copper matrix was first detected on the left side, accompanied by a small amount of dissolved zirconium. When the line-scan traverses through the interface, the zirconium signal sharply increases. When the scan enters the diamond fracture, the carbon signal increases markedly, and neither copper nor zirconium dissolved into the diamond particles. The residual zirconium in the copper matrix originated from the dissolution of zirconium layer by the molten copper at above melting point. After pure zirconium dissolved into the copper matrix, the inner ZrC layer remained on the diamond surface. The ZrC layer showed a distinct interphase between diamond and copper matrix (Fig. 5c). The thickness of ZrC layer was about 312.6 nm which was measured with the screen ruler software of scanning electron microscope.

Figure 6 shows the elemental distribution maps for the surface of a local fracture area. The regular

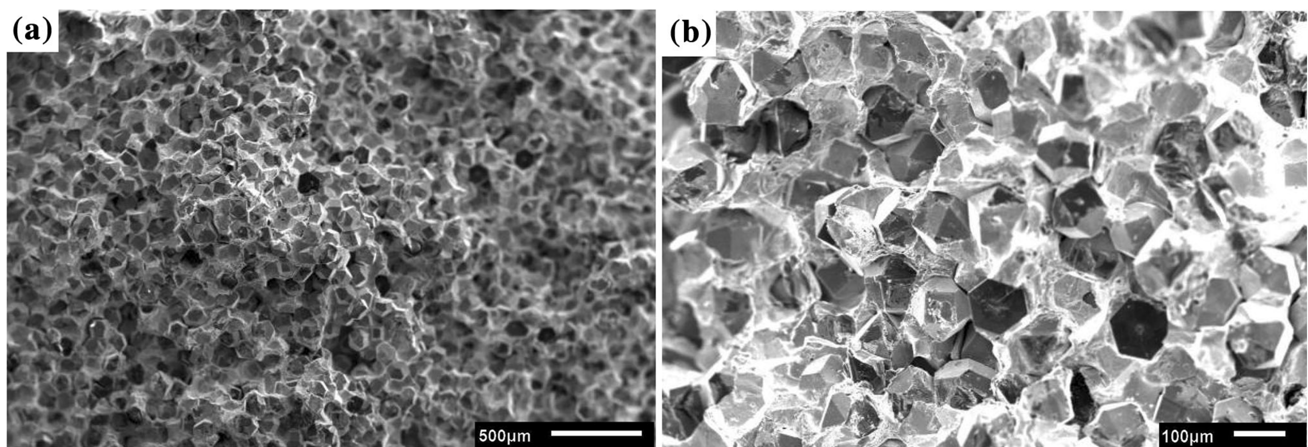


**Figure 4** SEM images of fracture surfaces of 65vol% diamond/Cu composites fabricated with double-layer coated diamond particles: **a** macroscopic fracture surface of diamond/Cu composites, and **b** fracture morphology in local regions.

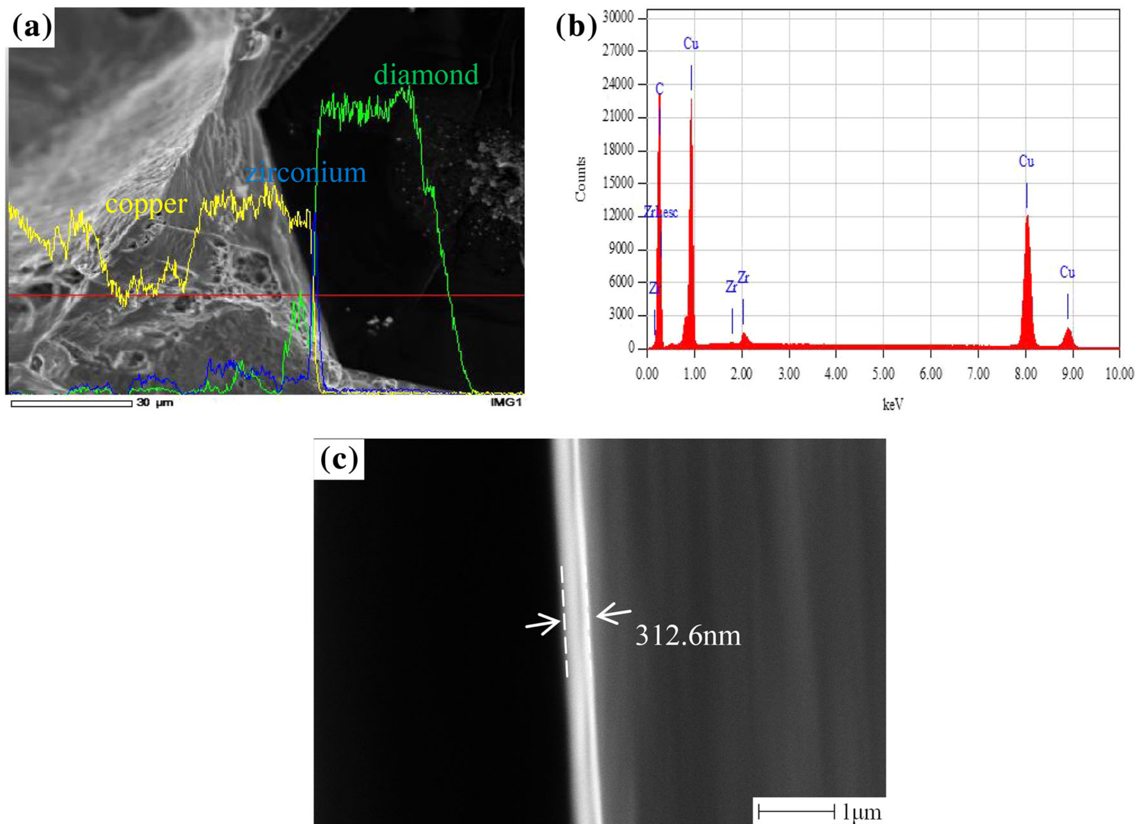


**Figure 5** EDS line-scanning analysis across the interface between diamond and copper: **a** SEM image for EDS line-scanning, **b** EDS spectrum corresponding to line-scanning and **c** the thickness of ZrC layer measured with screen ruler software.

hexagonal area with straight edges only exhibits carbon signal, and these diamond fractures were caused by intercrystalline failure. Along with the straight edges, zirconium was enriched as thin lines around the diamond surface. In contrast, the exposed diamond surface contained carbon, zirconium and copper (Fig. 6c), demonstrating a strong bonding between diamond particles, zirconium layer and copper matrix.

The thermal conductivities of diamond/Cu composites fabricated with double-layer particles containing different diamond contents are shown in Fig. 7. The detailed parameters for calculating TC are shown in Table 1. With increasing diamond volume fraction, the thermal conductivity rose steadily and reached maximum (720 W $m^{-1}$ $K^{-1}$) at the diamond content of 65 vol%. This value was higher than that of diamond/Cu composites fabricated by powder metallurgy [7, 11, 12] and infiltration methods [14, 15, 19, 21] (Table 2). When the diamond content increased to 70 vol%, the thermal property slightly declined because the copper layer was attenuated and densification was affected.

The interfacial thermal resistance of the zirconium carbide coating layer mainly consists of three parts: $R_T = R_{\mathrm{diamond/ZrC}} + R_{\mathrm{ZrC}} + R_{\mathrm{ZrC/Cu}}$. As for the theoretic calculation of interfacial thermal resistance between diamond surface and copper matrix, AMM is a standard model which considers such resistance as a function of phonon density on each material [7]. Based on the AMM model, the interfacial thermal resistance can be predicted with the intrinsic physical parameters of two media and calculated by combining the following two equations:

$$R = \frac{2(\rho_m v_m + \rho_d v_d)^2}{C_m \cdot \rho_m^2 \cdot v_m^2 \rho_d \cdot v_d} \left(\frac{v_d}{v_m}\right)^2 \quad (1)$$

$$v = \sqrt{G/\rho} \quad (2)$$

where $\rho$ is the density, $v$ is the Debye velocity, $C$ is the specific heat and $G$ is the shear modulus. Subscripts $m$ and $d$ represent the matrix and particle reinforcement, respectively.

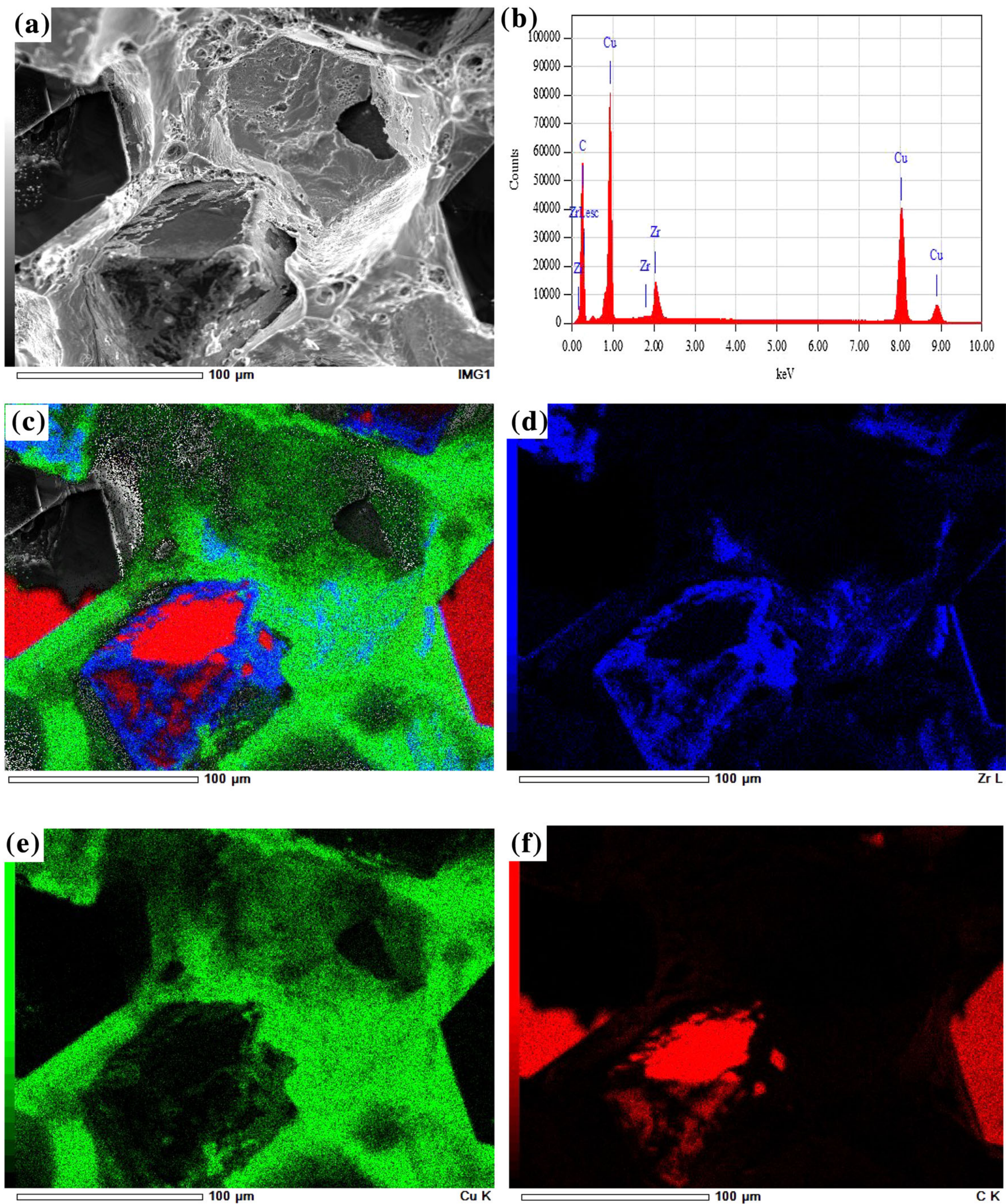


**Figure 6** EDS element mapping of the fracture surface of 65vol% diamond/Cu composites: **a** SEM image for subsequent element mapping, **b** EDS spectrum corresponding to the SEM image, **c** EDS mapping distributions of all elements on the fracture surface and **d**–**f** EDS mapping distributions of Zr, Cu and C, respectively.

In the calculation of the interfacial thermal resistance between diamond and ZrC layer ($R_{\mathrm{diamond/ZrC}}$), ZrC is assumed as the matrix and diamond is the reinforcement. To calculate such resistance between ZrC layer and copper ($R_{\mathrm{ZrC/copper}}$), copper is assumed as the matrix and ZrC is the reinforcement. By substituting the parameters of diamond, zirconium carbide and copper into the above formulas, $R_{\mathrm{diamond/ZrC}}$ and $R_{\mathrm{ZrC/Cu}}$ were calculated as $0.363 \times 10^{-8}$ and $0.544 \times 10^{-8}$ m$^2$ K W$^{-1}$, respectively.

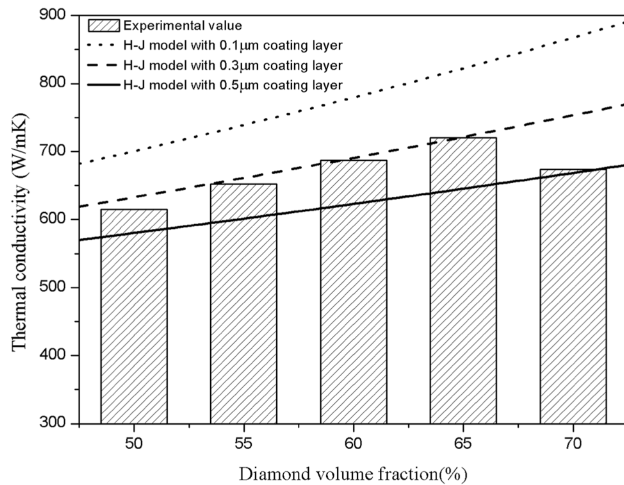


**Figure 7** Thermal conductivity of diamond/Cu composites with double-layer coated diamond particles based on the H–J model.

On the other hand, the thermal resistance of the ZrC layer itself is mainly affected by the coating thickness and can be predicted by $R = L/\lambda$, where $L$ is the thickness of the ZrC layer. By substituting $L = 0.1/0.3/0.5$ μm into the equation, respectively, we obtained the thermal resistances of ZrC layers with different thicknesses: $R_{ZrC} = 0.476 \times 10^{-8}$ m$^2$ K W$^{-1}$ ($L = 0.1$ μm), $R_{ZrC} = 1.429 \times 10^{-8}$ m$^2$ K W$^{-1}$ ($L = 0.3$ μm) and $R_{ZrC} = 2.381 \times 10^{-8}$ m$^2$ K W$^{-1}$ ($L = 0.5$ μm). Additionally, $R_{ZrC}$ is the major part of the interfacial thermal resistance. As the theoretical thickness of the ZrC layer varied from 0.1 μm to 0.5 μm, the total interfacial thermal resistance ($R_T$) increased significantly from $1.383 \times 10^{-8}$ to $3.288 \times 10^{-8}$ m$^2$ K W$^{-1}$. The thermal conductivity curve can be plotted by substituting the calculated $R_T$ value into the Hasselman–Johnson (H–J) formula below [18, 19]:

$$\lambda_c = \lambda_m \frac{[\lambda_d(1 + 2R_T\lambda_m/a) + 2\lambda_m] + 2V_d[\lambda_d(1 - R_T\lambda_m/a) - \lambda_m]}{[\lambda_d(1 + 2R_T\lambda_m/a) + 2\lambda_m] - V_d[\lambda_d(1 - R_T\lambda_m/a) - \lambda_m]} \quad (3)$$

where $\lambda$ refers to the thermal conductivity, $V$ is the volume fraction of reinforcement particles, $a$ is the average radius of reinforcement particles and $R_T$ is the interfacial thermal resistance between matrix and reinforcement particles. Subscripts $c$, $m$ and $d$ refer to the composite, matrix and reinforcement particles, respectively. The H–J formula, which takes into account all the factors that impact the composite thermal conductivity, is the most accurate model herein. With different $R_T$ values, the theoretical thermal conductivity curve varies considerably, as shown in Fig. 7.

The experimental values of diamond/Cu composites with different diamond volume fractions

**Table 1** Parameters for thermal conductivity calculation of diamond/Cu composites

| $V_d$ (vol%) | Density (g/cm$^3$) | Specific heat capacity (J g$^{-1}$ K$^{-1}$) | Thermal diffusivity (mm$^2$/s) | Thermal conductivity (W m$^{-1}$ K$^{-1}$) |
|---|---|---|---|---|
| 50 | 6.219 | 0.423 | 233.859 | 615.20 |
| 55 | 5.938 | 0.432 | 254.298 | 652.33 |
| 60 | 5.675 | 0.435 | 278.406 | 687.28 |
| 65 | 5.390 | 0.449 | 297.656 | 720.36 |
| 70 | 5.113 | 0.453 | 290.823 | 673.60 |

**Table 2** Thermal conductivities of diamond/Cu composites prepared by different methods

| Raw material | Preparation method | TC(W m$^{-1}$ K$^{-1}$) | References |
|---|---|---|---|
| Cr-coated diamond/Cu powder | P/M-SPS (37–43 MPa/930–950 °C/15–22 min) | 225 ~ 657 | [7] |
| $B_4C$-coated diamond/Cu powder | P/M-vacuum hot pressing (50 MPa/950 °C/20 min) | 500 ~ 665 | [11] |
| Diamond/Cu powder (bulk) | High-presssure high-temperature (5.3GPa/1200 °C/10 min) | 191 ~ 717 | [12] |
| Cr-coated diamond/Cu bulk | Pressureless infiltration(1250–1450 °C/30–110 min) | 350 | [14] |
| Ti-coated diamond/Cu bulk | Gas pressure infiltration (1 MPa/1150/15 min) | 716 | [15] |
| $Mo_2C$-coated diamond/Cu bulk | Vacuum pressure infiltration (20 MPa/1150 °C/5 min) | 550 ~ 608 | [19] |
| WC-coated diamond/Cu bulk | Vacuum pressure infiltration (20 MPa/1150 °C/5 min) | 658 | [21] |
| Cu–ZrC-coated diamond particles | High pressure(1.2GPa)/vacuum sintering(1100 °C/60 min) | 615 ~ 720 | This study |

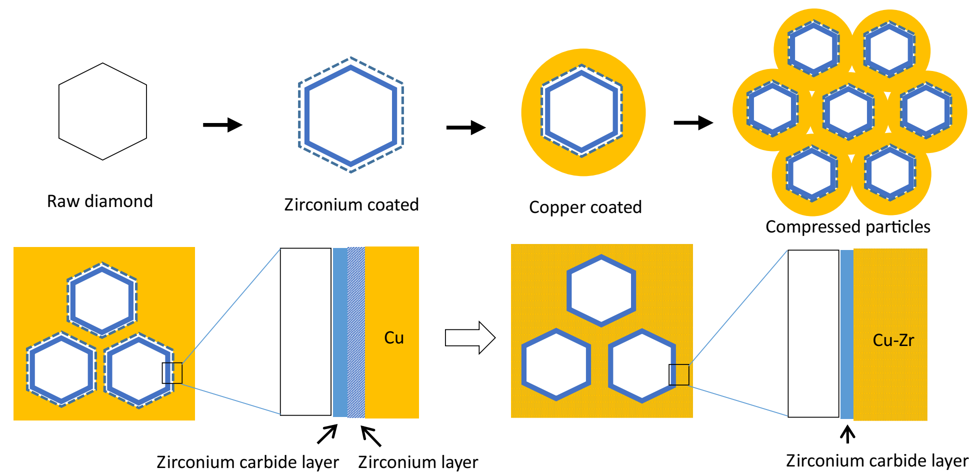


**Figure 8** Schematic diagram of coating process and variation of zirconium layer during sintering.

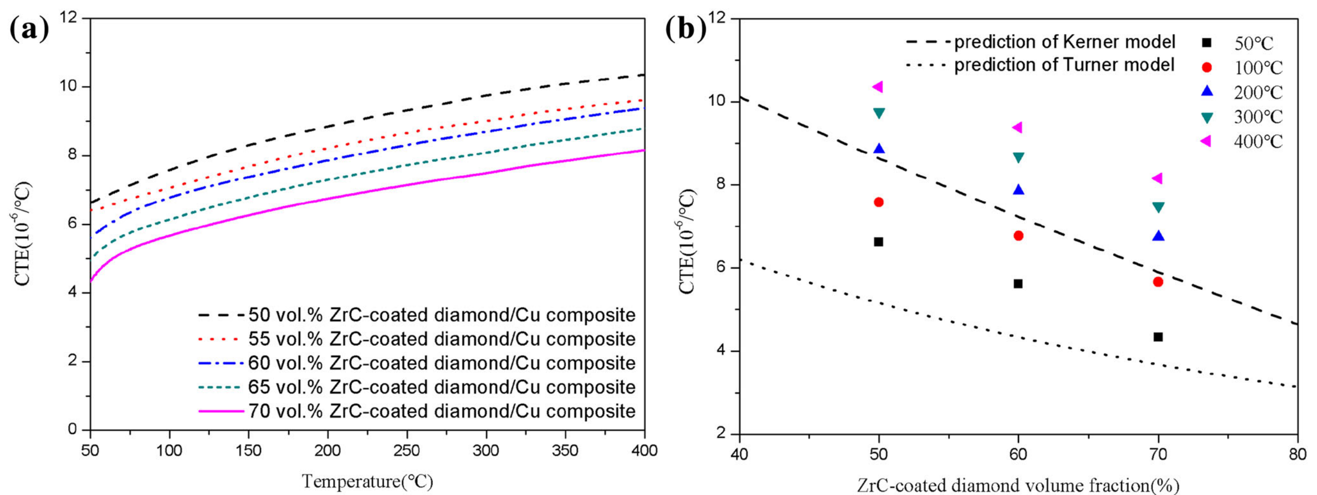


**Figure 9** CTE values of double-layer coated diamond/Cu composites: **a** CTE curves of diamond/Cu composites with increasing temperature, and **b** experimental CTE values compared with the value predicted by the Turner and Kerner model.

conform to the theoretical curve of 0.3-μm-thick coating layer. The zirconium layer was dissolved by molten copper (Fig. 8). Based on the XRD analysis of zirconium-coated diamond particles, the coating layer mainly consisted of two parts: a ZrC layer close to superficial diamond and a pure Zr layer covered thereon. When the copper matrix was heated at above melting point (1100 °C) and held for a period of time, the pure Zr outer layer gradually became thinner and dissolved into the copper matrix. According to theoretic calculation based on the H–J model, the interfacial thermal resistance plummeted as the zirconium coating layer was slightly attenuated. In addition, little zirconium coating layer dissolved, barely reducing the thermal property of the copper matrix.

A matching coefficient of thermal expansion with that of microelectronic device used at high and low cyclic temperatures is another important parameter for electronic packaging materials. Figure 9 shows the CTE curves of 50–70 vol% diamond/Cu composites with rising temperature from 50 to 400 °C. Clearly, CTE increased slowly as the temperature reached up to 400 °C. All the coefficients of thermal expansion had the same order of magnitude at below 400 °C. Particularly, the CTE variations of composites can be predicted by the typical Kerner and Turner model. When the temperature was below 100 °C, all CTE values of the diamond/Cu composites were between the two theoretical curves. As for 70 vol% diamond/Cu composite, CTE was as low as $4.33 \times 10^{-6}$/K, which can be attributed to both the homogeneous distribution of diamond particles and the strong interface bonding between these particles and copper matrix.

## Conclusions

In summary, diamond/Cu composites were fabricated by cold pressing and vacuum sintering with double-layer diamond particles. With this new method, copper was plated many times as the matrix to replace copper powders, giving homogeneously distributed diamond particles. The zirconium carbide inner layer effectively enhanced the interface bonding between the diamond surface and copper matrix. At above melting point, the zirconium layer was attenuated, thereby effectively reducing the interfacial thermal resistance. The thermal conductivity of 65 vol% diamond/Cu composite reached as high as 720 W $m^{-1}$ $K^{-1}$. When the diamond content increased to 70 vol%, an extremely low coefficient of thermal expansion ($4.33 \times 10^{-6}$/K) was obtained. With satisfactory thermo-physical properties, diamond/Cu composites fabricated by this new method can meet the demand of heat sink and be potentially eligible electronic packaging materials.

## Acknowledgements

This project is financially supported by the National Key R&D Program of China (2016YFB0301400) and the National Natural Science Foundation of China (Grant No. 51274040).

## References

[1] Molina JM, Narciso J, Weber L, Mortensen A, Louis E (2008) Thermal conductivity of Al–SiC composites with monomodal and bimodal particle size distribution. Mater Sci Eng A 480:483–488

[2] Zweben C (2002) Advanced materials for optoelectronic packaging. Electron Packag Prod 42:37–40

[3] Yoshida K, Morigami H (2004) Thermal properties of diamond/copper composite material. Microelectron Reliab 44:303–308

[4] Kidalov SV, Shakhov FM (2009) Thermal conductivity of diamond composites. Materials 2:2467–2495

[5] Bai H, Ma NG, Lang J, Zhu CX, Ma Y (2013) Thermal conductivity of Cu/diamond composites prepared by a new pretreatment of diamond powder. Compos Part B 52:182–186

[6] Chu K, Liu ZF, Jia CC, Chen H, Liang XB, Gao WJ, Tian WH, Guo H (2010) Thermal conductivity of SPS consolidated Cu/diamond composites with Cr-coated diamond particles. J Alloys Compd 490:453–458

[7] Ren SB, Shen XY, Guo CY, Liu N, Zang JB, He XB, Qu XH (2011) Effect of coating on the microstructure and thermal conductivities of diamond-Cu composites prepared by powder metallurgy. Compos Sci Technol 71:1550–1555

[8] Zhang C, Wang RC, Cai ZY, Peng CQ, Feng Y, Zhang L (2015) Effects of dual-layer coatings on microstructure and thermal conductivity of diamond/Cu composites prepared by vacuum hot pressing. Surf Coat Technol 277:299–307

[9] Wang HY, Tian J (2014) Thermal conductivity enhancement in Cu/diamond composites with surface-roughened diamonds. Appl Phys A 116:265–271

[10] Zhang C, Wang RC, Cai ZY, Peng CQ, Wang NG (2015) Low-temperature densification of diamond/Cu composite prepared from dual-layer coated diamond particles. J Mater Sci: Mater Electron 26:185–190

[11] Hu HB, Kong J (2014) Improved thermal performance of diamond–copper composites with boron carbide coating. J Mater Eng Perform 23:651–657

[12] Chen H, Jia CC, Li SJ (2012) Interfacial characterization and thermal conductivity of diamond/Cu composites prepared by two HPHT techniques. J Mater Sci 47:3367–3375. https://doi.org/10.1007/s10853-011-6180-6

[13] Rosinski M, Ciupinski L, Grzonka J, Michalski A, Kurzydlowski KJ (2012) Synthesis and characterization of the diamond/copper composites produced by the pulse plasma sintering (PPS) method. Diam Relat Mater 27–28:29–35

[14] Dong YH, He XB, Rafi UD, Xu L, Qu XH (2011) Fabrication and thermal conductivity of near-net-shaped diamond/copper composites by pressureless infiltration. J Mater Sci 46:3862–3867. https://doi.org/10.1007/s10853-011-5307-0

[15] Li JW, Zhang HL, Zhang Y, Che ZF, Wang XT (2015) Microstructure and thermal conductivity of Cu/diamond composites with Ti-coated diamond particles produced by gas pressure infiltration. J Alloys Compd 647:941–946

[16] Li JW, Wang XT, Qiao Y, Zhang Y, He ZB, Zhang HL (2015) High thermal conductivity through interfacial layer optimization in diamond particles Zr-alloyed Cu matrix composites. Scr Mater 109:72–75

[17] Li JW, Zhang HL, Wang LH, Che ZF, Zhang Y, Wang JG, Kim MJ, Wang XT (2016) Optimized thermal properties in diamond particles reinforced copper-titanium matrix composites produced by gas pressure infiltration. Compos Part A 91:189–194

[18] Ma SD, Zhao NQ, Shi CS, Liu EZ, He CN, He F, Ma LY (2017) $Mo_2C$ coating on diamond: different effects on

thermal conductivity of diamond/Al and diamond/Cu composites. Appl Surf Sci 402:372–383

[19] Kang QP, He XB, Ren SB, Zhang L, Wu M, Liu TT, Liu Q, Guo CY, Qu XH (2013) Preparation of high thermal conductivity copper-diamond composites using molybdenum carbide-coated diamond particles. J Mater Sci 48:6133–6140. https://doi.org/10.1007/s10853-013-7409-3

[20] Shen XY, He XB, Shu-Bin Ren SB, Zhang HM, Qu XH (2012) Effect of molybdenum as interfacial element on the thermal conductivity of diamond/Cu composites. J Alloys Compd 529:134–139

[21] Kang QP, He XB, Ren SB, Liu TT, Liu Q, Wu M, Qu XH (2015) Microstructure and thermal properties of copper-diamond composites with tungsten carbide coating on diamond particles. Mater Charact 105:18–23